

FRP STRENGTHENING OF SHEAR WALLS WITH OPENINGS

K. Behfarnia^{*a} and A.R. Sayah^b

^aDepartment of Civil Engineering, Isfahan University of Technology, Isfahan, Iran

^bSaze Andishan Pooya Consulting Engineers, Isfahan, Iran

Received: 12 September 2011, **Accepted:** 1 February 2012

ABSTRACT

Concrete shear walls are one of the main lateral resisting members in buildings. The functional requirements like architectural and even mechanical requirements entail that openings have to be installed in structural walls as well as floors. In this study, nonlinear static analysis was utilized to study the effects of fiber reinforced plastic (FRP) on the ultimate load capacity of concrete shear walls with openings using the finite element analysis software ABAQUS. In order to verify the accuracy of the numerical model, a comparison was done between the results of experimental and numerical analysis of a concrete shear wall. Subsequent to verification of the Finite Element Model (FEM), the effects of creating cut-off openings as well as strengthening effects of applying FRP have been studied. Whereas the numerical results show good correlation between the FEM and the experimental results of reinforced concrete (RC) shear walls, the numerical analysis represents a remarkable improvement in ultimate lateral load capacity of shear wall with opening strengthened using fiber reinforced plastic. The results obtained are presented in relative diagrams and tables.

Keywords: Shear wall; FEM; Abaqus; FRP; opening

1. INTRODUCTION

Earthquake resistant structures should be provided with lateral and vertical seismic force-resisting systems capable of transmitting forces to the foundations. Continuity and regular transitions are essential requirements to achieve adequate load paths [1]. Concrete shear walls are one of the main lateral resisting members in buildings because of their high in-plane rigidity. The functional requirements like architectural and even mechanical requirements entail that openings have to be installed in structural walls as well as floors. Generally, discontinuity regions in reinforced concrete walls like openings can cause stresses which cannot be classified in known patterns making the design difficult [2-5].

* E-mail address of the corresponding author: kia@cc.iut.ac.ir (K. Behfarnia)

Due to the high stress redistribution capability of concrete walls, creating small openings does not have a significant influence on the overall behavior of wall. However, creating large openings leads to significant reduction of wall rigidity and stiffness [1]. Thus, adequate measures should be taken to counteract these reductions. In the last decade, the use of fiber reinforced polymers (FRP) to strengthen existing structures has increased due to their excellent characteristics such as high resistance, durability, ease of installation and high strength to weight ratio [6-10]. Though a significant amount of research has been conducted on the use of fiber reinforced plastic for the strengthening and rehabilitation of reinforced concrete elements, there is little information on the strengthening of shear walls. One of the first projects using FRP strengthening of RC shear walls was reported in 1997 by Ehsani and Saadatmanesh [11]. They used FRP in order to retrofit a concrete building subjected to the Northridge earthquake. Another study on FRP strengthening of RC shear walls has been carried out by Lombard et al [12]. The purpose was to investigate the feasibility of CFRP strengthening and rehabilitation of reinforced concrete shear walls. In his studies four walls were tested in a quasi-static cyclic load sequence in predetermined load control steps up to the calculated yield load and then predetermined displacement control steps up to failure, respectively. The configuration of the CFRP strengthened system consisted of one or three sheets with fibers oriented either vertical or vertical and horizontal directions on both faces of the walls. Based on the test results, he developed an analytical model to predict the ultimate flexural capacity of plain reinforced concrete shear wall and walls strengthened or repaired with externally bonded fiber reinforced plastics based on the test results. Another study has been carried out by Sugiyama et al, where seismic behavior of non-structural reinforced concrete walls with openings strengthened using FRP composite sheets was studied [13]. He tested eight specimens of non-structural shear walls with the scale of 1/3. It was concluded that even if the bearing capacity of the non-structural walls increased, the global behavior of the frame remained the same. For a serviceability limit state (the deflection angle of doors and the residual crack width) a good enhancement was provided by the FRP strengthening [2, 13]. Another extensive experimental study was conducted by Antoniadis and Kappos on the strengthening of low-slenderness reinforced concrete (RC) walls designed to modern code provisions [14]. In this study the walls initially were subjected to cyclic loading to failure, and, subsequently, conventionally repaired and then strengthened using fiber-reinforced polymer (FRP) jackets. The results showed that the wall strengths increased from as low as 2 percent, to as high as 32 percent based on the anchorage conditions of the FRP strips. In 2005, Li et al analyzed the GFRP strengthening of shear walls in order to evaluate the accuracy of finite element method to predict the behavior of shear walls [15]. In this FEA model, a SPRING element was used to simulate the constraint deformation due to fiber reinforced polymer (FRP); also, a damaged plasticity-based concrete model was used to simulate the behavior of concrete under cyclic loading. The conformity of numerical and experimental results indicated the ability of finite element method to predict the behavior of FRP strengthening of shear walls. Despite these advances, more research is still required to study the structural behavior of strengthened walls with FRP, particularly with openings. Besides, most of the previous works only discussed experimental studies and analytical analyses but not finite element analysis and modeling. Consequently, in this study, the effects of applying FRP on the ultimate capacity of concrete shear walls with

openings were investigated by using the finite element analysis software ABAQUS. In this paper, the numerical model is calibrated and verified with experimental data from laboratory tests of plane RC shear walls. After verification of the FEM model, the effects of creating cut-off openings as well as the strengthening effects of applying FRP have been studied.

2. FE MODELING AND MATERIAL MODELS

2.1 Overview of the experimental reference model

In order to confirm the applicability of the proposed numerical models which are used in this study, experimental results from one of the RC shear walls specimens tested by Lefas [16, 17] et al is used. The wall was 750 mm wide, 750 mm high and 70 mm thick and monolithically was connected to an upper and lower beam. The upper beam (1150mm long, 150 mm deep and 200 mm thick) functioned as both the element through which axial and horizontal loads were applied to the walls and as a cage for anchorage of the vertical bars. The lower beam (1150 mm long, 300 mm deep and 200 mm thick) was utilized to clamp the specimens down to the laboratory floor [16, 17]. The location of hydraulic jacks and the details of bar locations are shown in Figure 1a and 1b, respectively. The material properties and percentage of reinforcement are given in Table 1.

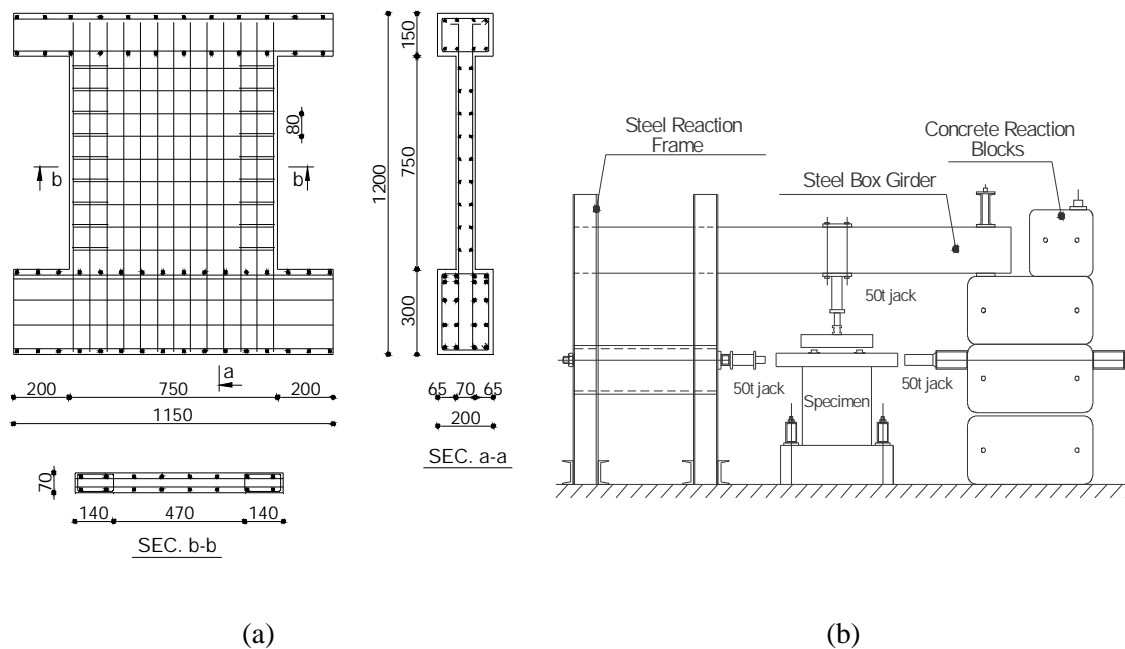


Figure 1. (a) Rebar details and wall dimensions (mm); (b) Test setup [13, 14]

Table 1: Mechanical properties of materials ^a

Type	Yielding strength (F_y) and ultimate stress (F_u) of steel (MPa)		Cube strength of concrete (MPa)	Elastic modulus of concrete (MPa)	Tensile strength of concrete (MPa)	Vertical load (kN)	Reinforcement percentage				
	Diameter	F_y					F_u	ρ_{hor} percent	ρ_{ver} percent	ρ_{nex} percent	ρ_s percent
SW-13	f4	420	490	40.6	27600	3.2	355	1.10	2.40	3.10	1.20
	f6.25	520	610								
	f8	470	565								

^a Modulus of elasticity of steel is 21000 MPa and Poisson's ratio of concrete and steel are considered to be 0.2 and 0.3, respectively. ρ_{nex} = ratio of main flexural reinforcement to gross concrete area of edge element; ρ_{hor} = ratio of horizontal bars to gross concrete area of vertical section of wall web; ρ_{ver} = ratio of vertical web bars to gross concrete area of horizontal section of wall web; ρ_s = ratio of effective volume of confinement bars to the volume of the core.

2.2 Finite Element Model

In this study, nonlinear analysis was utilized using the finite element analysis software ABAQUS. The concrete wall was modeled using 8-node 3-D solid elements (C3D8R) which had three degrees of transitional freedom in each node. In the ABAQUS software, there are two possible ways to model reinforcement bars in three dimensional concrete elements. Reinforcement bars can be modeled either as an embedded rebar layer or as truss elements. The first method is better for regular distributed reinforcement [18]. However, considering arrangement of reinforcements in boundary elements, it is better to model discrete reinforcement in the form of two dimensional truss elements (T3D2) which are embedded in C3D8R solid elements. The effects associated with the rebar-concrete interface, like bond slip and dowel action, are not considered by this model. As a result, these effects may model approximately by introducing some "tension stiffening" into the concrete modeling. External FRP reinforcement is modeled using 4-node shell elements with orthotropic behavior. It is worthwhile to mention that in ABAQUS STD analyses are performed using 8-Gauss integration points for solid elements and 4-Gauss integration points for shell elements, with 2-Gauss integration points over the thickness. The boundary condition of the base of the wall was simulated as fixed end. In order to prevent out-of-plane displacement, proper roller supports were placed at the mid surface of the model. Moreover, in order to simulate the loading conditions of the control wall, a vertical pressure load was applied on the top beam to simulate the vertical load; lateral displacement was applied on a steel plate at the top beam to simulate the lateral displacement.

2.3 Material Properties and Constitutive Models

This study involves modeling of steel reinforcing bars, concrete and FRP. However, constitutive models are available in the ABAQUS material library, but their input material properties and associated constitutive models are briefly discussed. For steel a bilinear model with strain hardening is used to determine the behavior of steel in tension and compression. Full bond between steel and concrete is assumed. The support plate which is used to apply the lateral displacement was considered to behave in a linearly elastic manner. The constitutive model used to analyse the concrete was a concrete damaged plasticity model which is a continuum,

plasticity-based, damage model. It assumes that the main two failure mechanisms of concrete are tensile cracking and compressive crushing. In addition, it assumes when the concrete specimen is unloaded from any point on the strain softening branch of the stress-strain curves, the unloading response is weakened which means the elastic stiffness of the material appears to be damaged (or degraded). The degradation of the elastic stiffness is characterized by two damage variables in tension and compression stress which can take values from zero, representing the undamaged material, to one, which represents total loss of strength. The model makes use of the yield function of Lubliner et al. with the modifications proposed by Lee and Fenves to account for different evolution of strength under tension and compression. The yield surface is controlled by two hardening variables, one in tension and one in compression [18]. For defining the yield function two parameters are required; the first parameter, which reflects the behavior of concrete under biaxial stress conditions, is the ratio of initial equibiaxial compressive strength to uniaxial compressive strength σ_{b0}/σ_{c0} . The concrete under combinations of biaxial stress exhibits behaviors which are different from those under uniaxial loading conditions by the effects of Poisson ratio and microcrack confinement [19]. In the biaxial compression state of stress, concrete exhibits an increase in compressive strength of up to 25 percent of the uniaxial compressive strength [20]. In the equibiaxial state of stress, the concrete compressive strength (σ_{b0}) is approximately 1.16 times greater than the uniaxial concrete compressive strength (σ_{c0}). The second parameter is the ratio of the second stress invariant on the tensile meridian to that on the compressive meridian at initial yield for any given value of the first stress invariant such that the maximum principal stress is negative K_c the default values in ABAQUS were used $2/3$. The concrete damaged plasticity model assumes nonassociated potential plastic flow. The flow potential G used for this model was the Drucker-Prager hyperbolic function. This flow potential, which is continuous and smooth, ensures that the flow direction is always uniquely defined. For this function, a couple of parameters must be defined; the uniaxial tensile stress at failure, the dilation angle w and the eccentricity ε which is a parameter that defines the rate at which the function approaches the asymptote. The default flow potential eccentricity values in ABAQUS is $\varepsilon = 0.1$ [10,18]. In order to reduce the mesh sensitivity of the FEM, the postfailure behavior of concrete in tension must be provided. This can help to account for the effects associated with the rebar-concrete interface such as bond slip. The postfailure behavior can be defined by means of a stress-strain relationship or by applying a fracture energy cracking criterion. In this study, the behavior of concrete in tension is defined by means of trilinear stress-strain relation with an ascending branch until the first crack and a bilinear softening branch after cracking which is introduced by [18]. The choice of these parameters is important and they should be calibrated to a particular case. In this study, the FRP is considered as a linear elastic material until failure and the interaction between the concrete and the FRP is modeled without considering debonding.

2.4 Parameter to Identify Debonding in FEA Study

In order to control the debonding in FRP, the effective FRP strain at failure is calculated by means of the equations provided by ACI 440 [21]. In addition, FRP strain was controlled in each step of the analysis in order to identify debonding and rupture in the FEA study.

2.5 Numerical Procedure

In this study, a displacement-controlled incremental loading method was adopted and an iterative solution procedure based on the modified Newton–Raphson method was employed

in order to simulate nonlinear behavior of FEM using the ABAQUS software.

3. VERIFICATION STUDY

The validity of the proposed material constitutive models for steel, concrete and FRP were verified by testing against experimental data. The results of the verification study, Figure 2, demonstrated that the numerical model fitted with acceptable accuracy the experimental results of the reference wall. For instance, the measured maximum lateral force and corresponding displacement in the reference wall were 330kN and 8.88mm, respectively [16,17]. On the other hand, the numerical predictions obtained for maximum lateral force and corresponding displacement were 314 kN and 9.74 mm, respectively. Moreover, cracking patterns in the FE model fitted with the the experimental results of the reference wall. It is worthwhile to mention that the concrete damaged plasticity model does not have the notion of cracks developing at the material integration point. However, in order to show cracking patterns we can show maximum principal plastic strain in FE analysis, because we can assume that cracking initiates at points where the tensile equivalent plastic strain is greater than zero. After verification of the finite element method with the proposed reference model, in order to study the effects of cut-off openings, several arrangements of square openings with a variety of dimensions were created in various heights in the reference wall model. The models were divided into three main groups B, M, and T based on the opening location. Figure 3 shows the geometry of the wall and arrangements of openings. All models of group M had openings at the mid-height of the wall whereas models of group B, and T had openings at the bottom and top of the wall, respectively. The opening size was either $L/4$, $L/3$, or $L/2$ (L corresponded to the length of the wall); consequently, in the finite element model, the steel reinforcement intercepted by the opening was cut. Table 2 illustrates the details of openings and the analysis results. Figure 4a, 4b and 4c show the force-displacement curves of reference wall with opening at the mid-height, at the top of the wall and the support, respectively.

Table 2: Details and results of forming openings in the reference wall

Model	Y (mm)	$X_1=Y_1$ (mm)	Opening area to wall area (percent)	F_{max} (kN)	Capacity reduction (percent)
SW-L/4-B	93.75	187.5	6.25	228.64	27.1
SW-L/4-M	375	187.5	6.25	260.09	17.1
SW-L/4-T	656.2	187.5	6.25	282.99	9.8
SW-L/3-B	125	250	11.11	197.28	37.1
SW-L/3-M	375	250	11.11	209.3	33.3
SW-L/3-T	625	250	11.11	255.33	18.6
SW-L/2-B	187	375	25	130.95	58.3
SW-L/2-M	375	375	25	130.70	58.4
SW-L/2-T	562.5	375	25	119.65	61.9

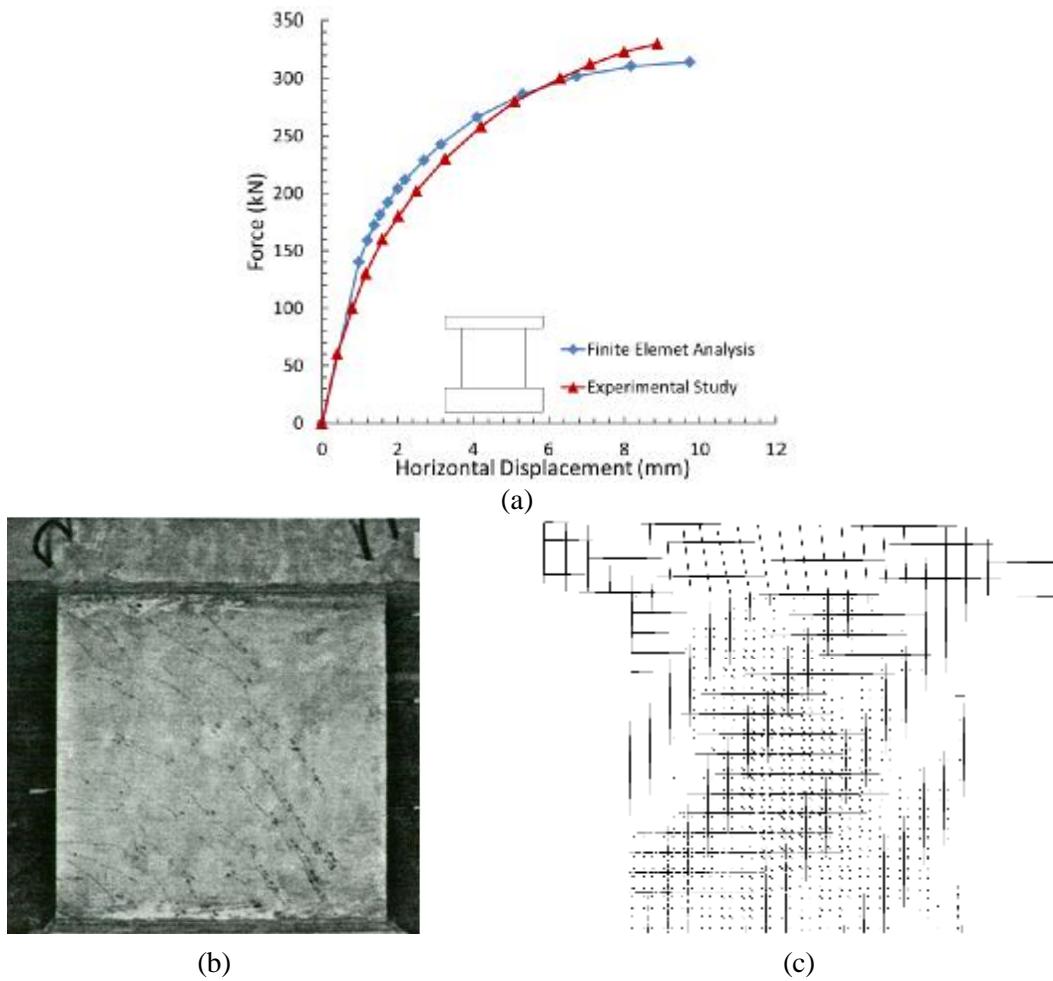


Figure 2. (a) Load–top displacement curve from experimental and numerical analysis of reference shear wall; (b) cracking patterns in reference wall [16,17]; (c) cracking patterns in numerical model

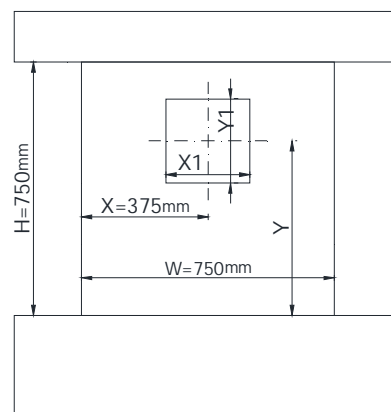


Figure 3. Geometry of the wall

As it can be seen in table 2 and Figure 4, creating an opening with the area equal to 6.25 or 11.11 percent of the total area of the wall will cause reduction in the ultimate capacity of wall from 9.8 percent (In model SW-L/4-T) up to 37.1 percent (In model SW-L/3-B). However, by increasing the area of openings to 25 percent, a capacity reduction from 58.3 percent to 61.9 percent was observed based on the location of the openings. It should be noted that in models with small openings, the location of opening plays a significant role; however in models with large openings, the wall capacity was not significantly affected by changing the location of the opening; because large openings will affect the integrity and vary the wall behavior to a frame action in which overturning moments are resisted by an axial compression–tension couple across the wall piers rather than by the individual flexural or shear action of the walls [22]. It can be inferred from table 2 that changing the location of the opening from top to bottom of SW-L/2 wall resulted in 5.8 percent change in capacity reduction; however, in SW-L/4 wall this number is equal to 63.8 percent.

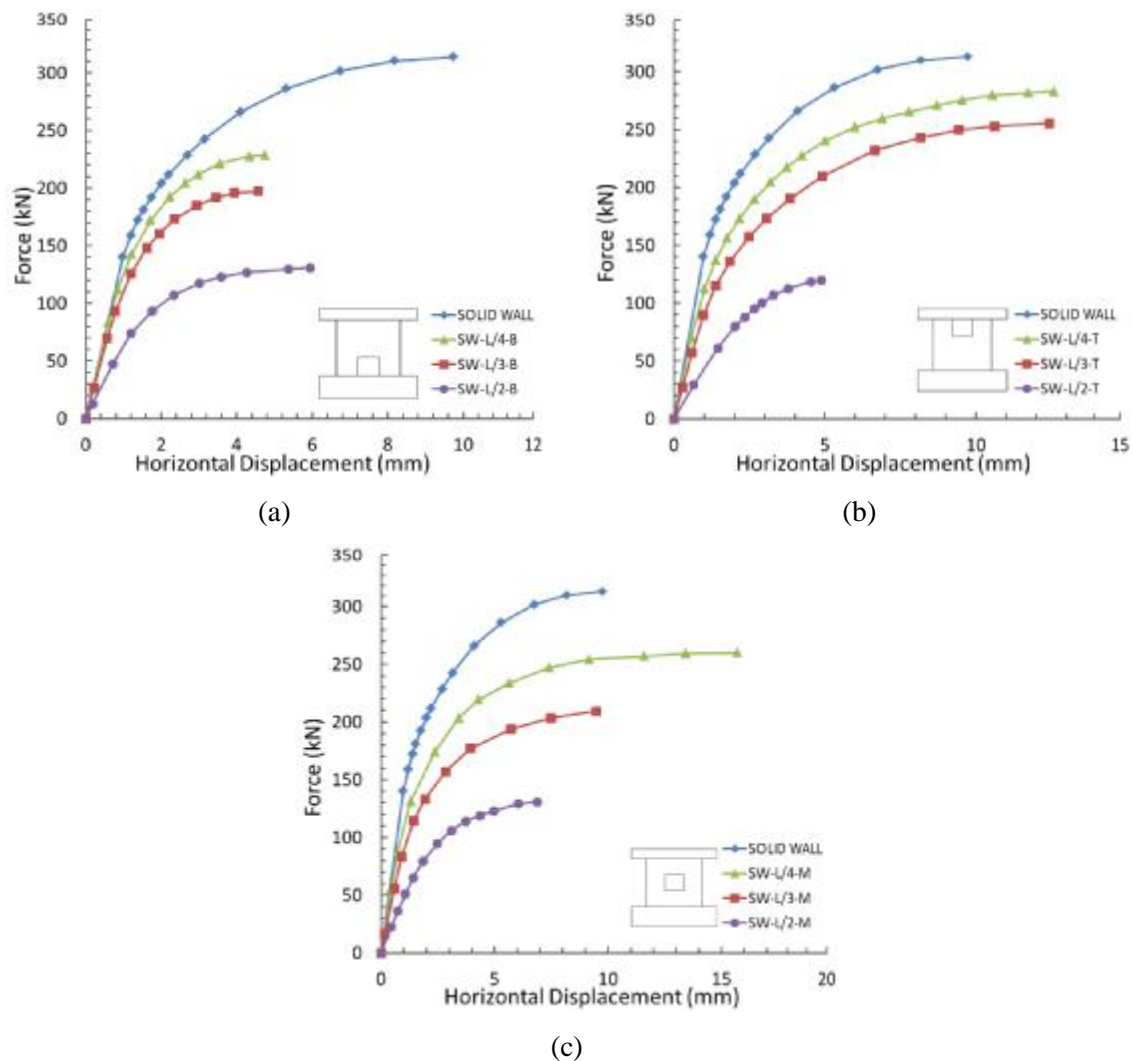


Figure 4. Load–top displacement curve from: (a) group B; (b) group T; (c) group M

4. STRENGTHENING TECHNIQUE

The CFRP scheme used as external strengthening is shown schematically in Figure 5. The strengthening technique consists of unidirectional CFRP wraps with the fibers oriented horizontally for the top and bottom areas of the opening with the width of $Y1/2$ ($Y1$ is the opening height) and also two piers. The thickness of CFRP used to strengthen the shear walls are C1, C2 and C3 which are equal to 0.05, 0.08 and 0.12 mm, respectively. Table 3 and 4 illustrate mechanical properties of the CFRP and names of the models which are based on the location of the opening as well as the thickness of laminates, respectively.

Table 3: Mechanical properties of CFRP

Longitudinal Elastic Modulus (GPa)	281
Transverse Elastic Modulus (GPa)	7.71
Ultimate Strain	0.015
Ultimate Stress (MPa)	4215

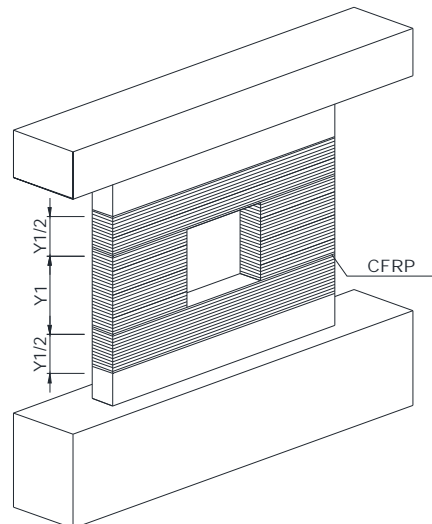


Figure 5. CFRP scheme used as external strengthening

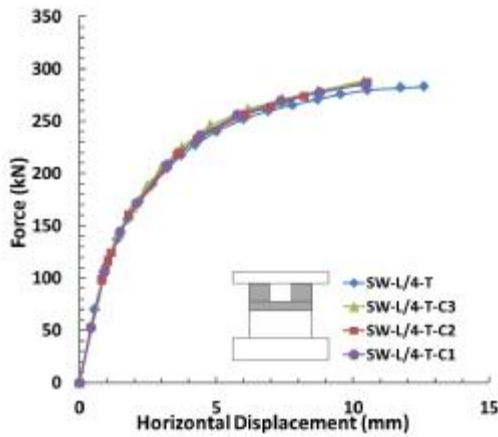
5. NUMERICAL RESULTS OF FINITE ELEMENT ANALYSIS OF STRENGTHENED WALLS

The analysis results of the strengthened walls and the load versus top horizontal displacement curve are presented in Figure 6 and Table 4. As can be seen, the effectiveness of the CFRP strengthening method in improving the capacity of walls is related to the thickness of laminates as well as the dimensions and location of openings in the walls.

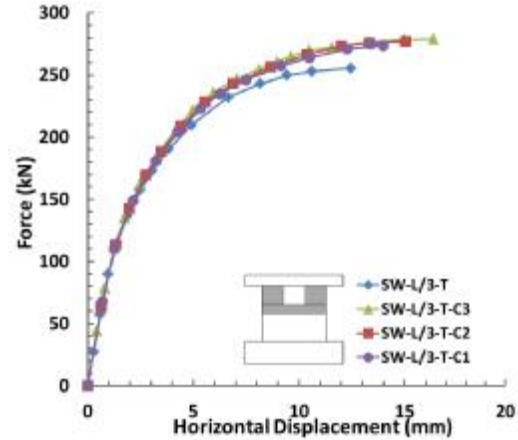
Table 4: Results of CFRP strengthened models

Model	F_s (kN)	F_s/F_{NS}	Model	F_s (kN)	F_s/F_{NS}	Model	F_s (kN)	F_s/F_{NS}
SW-L/4-B-C1	242	1.06	SW-L/3-B-C1	211	1.07	SW-L/2-B-C1	141	1.08
SW-L/4-B-C2	246	1.08	SW-L/3-B-C2	215	1.09	SW-L/2-B-C2	149	1.14
SW-L/4-B-C3	251	1.1	SW-L/3-B-C3	220	1.12	SW-L/2-B-C3	154	1.17
SW-L/4-M-C1	264	1.02	SW-L/3-M-C1	215	1	SW-L/2-M-C1	158	1.2
SW-L/4-M-C2	274	1.05	SW-L/3-M-C2	225	1.05	SW-L/2-M-C2	165	1.26
SW-L/4-M-C3	284	1.09	SW-L/3-M-C3	240	1.12	SW-L/2-M-C3	171	1.31
SW-L/4-T-C1	286	1.01	SW-L/3-T-C1	275	1.07	SW-L/2-T-C1	154	1.29
SW-L/4-T-C2	286.8	1.015	SW-L/3-T-C2	277	1.08	SW-L/2-T-C2	160	1.34
SW-L/4-T-C3	288	1.02	SW-L/3-T-C3	279	1.09	SW-L/2-T-C3	166	1.39

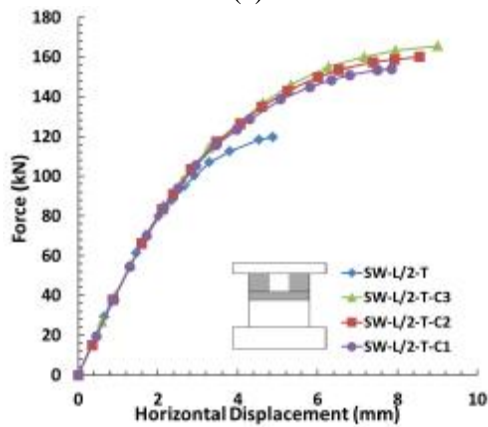
F_s/F_{NS} is the ratio of ultimate lateral load of the strengthened model to the ultimate lateral load of the unstrengthened model.



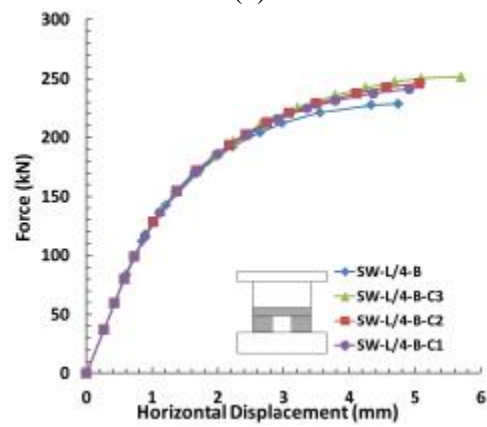
(a)



(b)



(c)



(d)

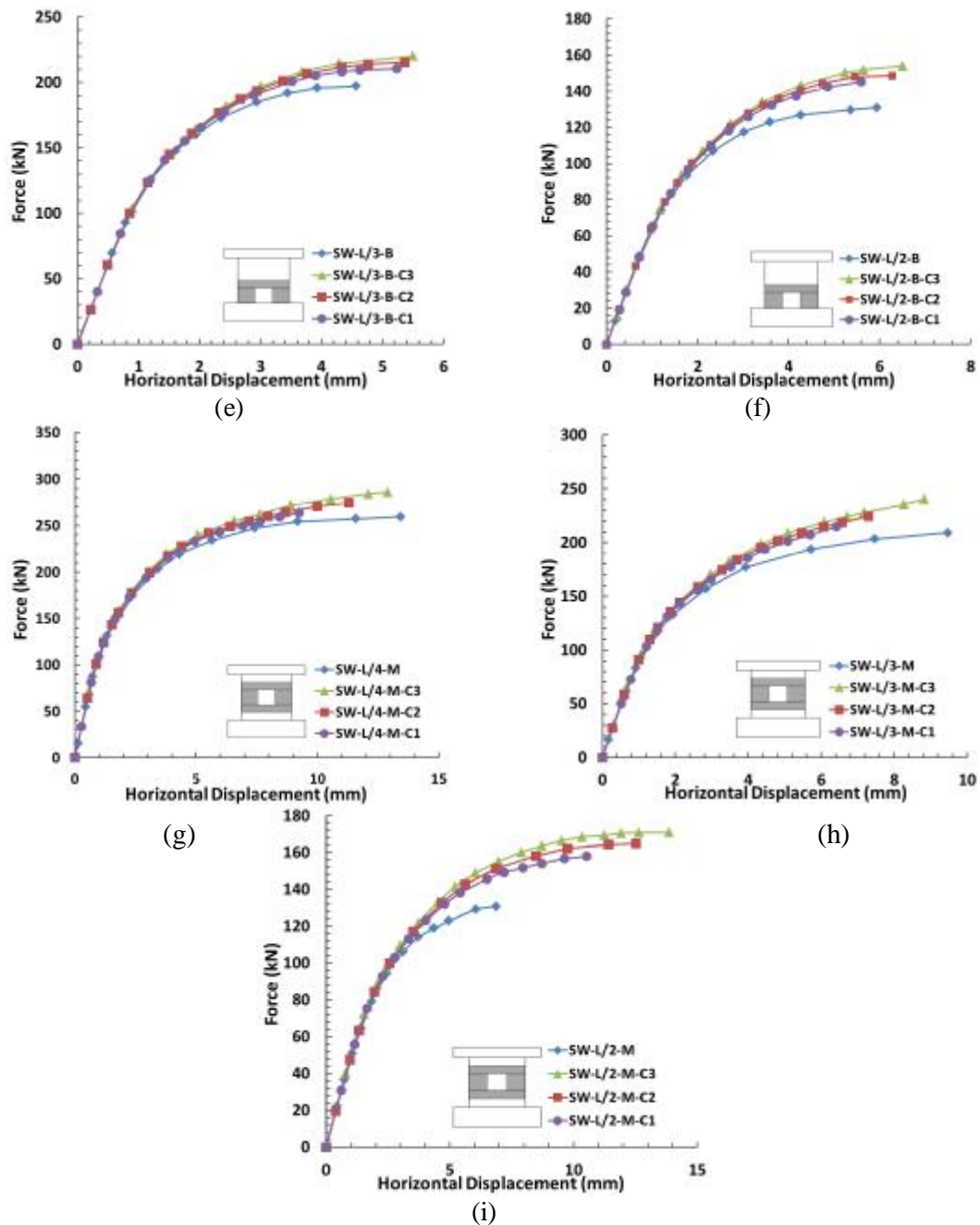


Figure 6. Load-top displacement curve from numerical analysis of strengthened models

For example highest effect on ultimate load capacity was observed in the SW-L/2-T-C3 model, Figure 6-c, (39%) which had a square opening at the top of the wall with the dimension of 370 mm, 25 percent of total surface area of the walls, strengthened with a layer of 0.12 mm laminate. On the other hand, the lowest effect on ultimate load capacity was observed in the SW-L/3-M-C1 model, Figure 6-h, (1%) which had a square opening with the

dimension of 250 mm in the mid-height of the web strengthened with one layer of 0.05 mm CFRP laminate. As can be seen in table 4, in models with the area of 25 percent of the total wall area, increasing the CFRP laminate thickness leads to increasing the maximum force and its corresponding displacement; while increasing the thickness of CFRP laminate, in models with smaller openings, mostly increased the displacement corresponding to the maximum force.

It is worthwhile to mention that in all strengthened models, the failures of the walls were neither rupture nor debonding of the CFRP.

6. CONCLUSIONS

The main two objectives of this paper are studying the effects of creating openings in shear walls and the potential use of externally bonded CFRP sheets for strengthening of RC shear walls with openings. Based on test results the following conclusions can be drawn:

1. Comparison between the experimental and numerical results indicated the ability of the finite element method procedure to give a reasonable prediction for behavior of RC shear walls.
2. Creating openings with the area equal to 11.11 percent of the total wall area or less resulted in a load capacity reduction of about 37.1 percent.
3. The failures of RC shear walls with openings in which the load path is disrupted by openings were dependent primarily on the opening sizes and locations. However, increasing the area of openings up to 25 percent (large opening) of total area of the walls lead to the a capacity reduction up to 61.9 percent. Moreover, in models with large openings, changing the location of the opening in the height of the walls did not have a significant effect on the wall ultimate load capacity. The primary reasons for this reduction is because the opening changed the integrity of shear walls to a frame action in which the lateral load resisting behavior changed to one where overturning moments were resisted partially by an axial compression–tension couple across the wall system rather than by the individual flexural action of the walls.
4. Shear strengthening around the openings of RC shear walls can remarkably increase the wall capacity, based on the size and location of the opening. The capacity gain caused by FRP sheets was in the range of 1 percent to 39 percent. The capacity gain was highest (39 percent) when the opening was located at the top of the walls. Only a strength gain of 6 percent was observed for the walls with bottom openings.
5. The failures of strengthened RC shear walls with openings, as well as unstrengthened walls, were dependent primarily on the thickness of FRP as well as the location and size of openings. In models with a large opening, increasing the CFRP plate thickness lead to increasing the ultimate load and its corresponding displacement; however, in models with smaller openings, increasing the thickness of CFRP plate mostly increased the displacement corresponding to the ultimate load.
6. CFRP strengthening had the highest effect on ultimate load capacity of models which had openings with the size of 25 percent of the total surface area of the walls in comparison to respective unstrengthened walls (up to 39 percent capacity increase). In the walls with the opening size of 11.11 percent and 6.25 percent of total surface area

of the walls a maximum increase in capacity up to 12 percent was observed.

7. In all strengthened models, the failures of the walls were neither rupture nor debonding of the CFRP.

REFERENCES

1. Elnashai A, Sarno L. *Fundamentals of Earthquake Engineering*, John Wiley, New York, 2008.
2. Sas G. *FRP Shear Strengthening of RC Beams and Walls*, Department of Civil, Mining and Environmental Engineering, Luleå University of Technology, Licentiate Thesis, 2008.
3. El-Dakhkhni WW, George S, Shedid MT. Seismic retrofit of concrete block wall intersections using composite laminates, *Journal of Reinforced Plastics and Composites*, No. 11, **20**(2010) 1609-25.
4. Torki Harcheganiu ME, Talaei Taba B, Farahbod F. Effect of opening dimensions on the relative flexural operation of coupled shear walls, *Asian Journal of Civil Engineering*, No. 3, **13**(2012) 417-27.
5. Bozdogan KB. A method for free vibration analysis of stiffened multi-bay coupled shear walls, *Asian Journal of Civil Engineering*, No. 6, **7**(2006) 639-49.
6. Bhinia D, Prakash V, Pandey AD. A procedure for evaluation of coupling beam characteristics of coupled shear walls, *Asian Journal of Civil Engineering*, No. 3, **8**(2007) 301-14.
7. Sadeghian P, Rahai AR, Ehsani M. Effect of fiber orientation on compressive behavior of CFRP-confined concrete columns, *Journal of Reinforced Plastics and Composites*, No. 9, **29**(2010) 1335-46.
8. Ng SC, Lee A. Study of flexural behavior of reinforced concrete beam strengthened with carbon fiber-reinforced plastic (CFRP), *Journal of Reinforced Plastics and Composites*, No. 10, **21**(2002) 919-38.
9. Tanarlan HM, Ertutar Y. The effects of CFRP strips for improving shear capacity of RC beams, *Journal of Reinforced Plastics and Composites*, No. 12, **27**(2008) 1287-308.
10. Enochsson O, Lundqvist J, Taljsten B, Rusinowski P, Olofsson T. CFRP strengthened openings in two-way concrete slabs: an experimental and numerical study, *Construction and Building Materials*, No. 4, **21**(2002) 810-26.
11. Ehsani MM, Saadatmanesh M. Fiber composites: an economical alternative for retrofitting earthquake-damaged precast-concrete walls, *Earthquake Spectra*, No. 2, **13**(1997) 225-41.
12. Lombard J. *Seismic Strengthening and Repair of Reinforced Concrete Shear Walls Using Externally Bonded Carbon Fiber Tow Sheets*, Department of Civil and Environmental Engineering, Carleton University, Master of Engineering thesis, 1999.
13. Sugiyama T, Uemura M, Fukuyama H, Nakano K, Matsuzaki Y. Experimental study on the performance of the RC frame infilled cast-in-place on-structural RC walls retrofitted by using carbon fiber sheets, *Proceedings of the Twelfth World Conference on Earthquake Engineering*, New Zealand Society for Earthquake Engineering, Silverstream, New Zealand, Paper No. 2153, 2000.

14. Antoniadis KK, Salonikios TN, Kappos AJ. Cyclic tests on seismically damaged reinforced concrete walls strengthened using fiber-reinforced polymer reinforcement, *ACI Structural Journal*, No. 4, **100**(2003) 510-8.
15. Li ZJ, Balendra KH, Tan, KH. *Finite Element Modeling of Cyclic Behavior of Shear Wall Structure Retrofitted Using GFRP*, ACI-SP-230-74, 2005.
16. Lefas ID, Kotsovos MD, Ambraseys NN. Behavior of reinforced concrete structural walls: strength, deformation characteristics, and failure mechanism, *ACI Structure Journal*, No.1, **87**(1990) 23-31.
17. Lefas ID. Behavior of Reinforced Concrete Structural Walls and its Implication for Ultimate Limit State Design, Imperial College, University of London, PhD thesis, 1988. ABAQUS theory manual and users' manual, version 6.8, 2008.
18. Kwak H-G, Kim D-Y. Nonlinear analysis of RC shear walls considering tension-stiffening effect, *Computers and Structures*, **79**(2001) 499-517.
19. Kupfer H, Hilsdorf HK, Rusch H. Behavior of concrete under biaxial stresses, *ACI Structural Journal*, No. 8, **66**(1969) 656-66.
20. ACI 440. *Guide for the Design and Construction of Externally Bonded FRP Systems for Strengthening Concrete Structures*, ACI 440.2R-08, American Concrete Institute, Farmington Hills, MI, 2008.
21. Lu X, Chen Y. Modeling of coupled shear walls and its experimental verification, *Journal of Structural Engineering*, No. 1, **131**(2005) 75-84.